Int. J. Electrochem. Sci., 8 **(2013)** 9629 - 9643

International Journal of
ELECTROCHEMICAL
SCIENCE
www.electrochemsci.org

Application of Highly Surface Active Cationic Surfactants Based on Rosin as Corrosion Inhibitor for Tubing Steel During Acidization of Petroleum Oil and Gas Wells

Ayman M. Atta[*], *Gamal A. El-Mahdy, Amro K. F. Dyab, and Hamad A. Allohedan*

King Saud University, Chemistry Department, College of Science, P.O.Box - 2455, Riyadh - 11451, Saudi Arabia
[*]E-mail: aatta@ksu.edu.sa

Received: 13 May 2013 / *Accepted:* 10 June 2013 / *Published:* 1 July 2013

Rosin, a robust inexhaustible raw material from pine tree has attracted much attention due to its utilization as a feedstock for the preparation of cationic surfactants. Maleopimaric acid (MPA), one of most important rosin derivative obtained from the Diels-Alder reaction between the gum rosin and maleic anhydride which can be obtained with low cost and high purity and it used as intermediate compound for the preparation of cationic surfactants. MPA was reacted with oxalyl chloride and 2-diethylethanolamine to prepare rosin ester which quaternized with hexadecylbromide to obtain QRMAE cationic surfactant. The structure and properties of these rosin derivatives were characterized by FT-IR, and ^{1}H NMR. The results showed that MPA and QRMAE was high purity. The surface activity of the prepared QRMAE surfactant was evaluated in water and 1 M HCl to measure the micellization and adsorption of the prepared surfactants at water/air interface. The results showed that cationic derivative inhibited corrosion of carbon steel and the extent of its inhibition was concentration dependent. Potentiodynamic polarization investigations revealed that cationic acted as a mixed-type inhibitor. The inhibition efficiency increases with the concentration of cationic to attain 92 % at 250 ppm.

Keywords: Tubing Steel; corrosion; rosin; cationic surfactants; impedance and polarization techniques.

1. INTRODUCTION

It is well known that, the mild steel is widely used of in different petroleum applications, such as down hole tubular, flow lines and transmission pipelines. Moreover, corrosion problems may be occurred in numerous systems within the petroleum industry. Acidization of petroleum oil and gas reservoir stimulation technique is probably the most widely used work over and for increasing well

productivity [1]. The most common acids are hydrochloric, hydrofluoric, acetic, formic, sulfamic, and chloro acetic acids. Among of these various acids, hydrochloric acid solutions are widely used for stimulating carbonate-based reservoirs like lime stone and dolomite [2]. Moreover, hydrochloric acid solutions are widely used in petroleum for cleaning and descaling of iron and steel alloys. So that, highly surface active modified cheap organic corrosion inhibitors are highly recommended to inject in these acid media to reduce the corrosion rate of metallic materials [3-5]. The efficiency of corrosion inhibitors is affected by definite physico-chemical characteristics of the molecule such as functional groups, and the electronic structure of the molecule [6–8].

Rosin, being one of the important renewable resources, has excellent solubility and ready availability [9]. However, this renewable raw material is highly recommended to apply in the production of new materials which attributed to its cheap price and low toxicity when compared to the petroleum-based materials [10, 11]. Thus, rosin has received increasing attention as a raw material for the preparation of some new polymers with specific chemical structures and valuable properties [12]. We started to modify rosin chemical structure which can be converted to highly surface active materials to apply as additives for petroleum crude oil applications and used as corrosion inhibitors [13-21]. The aim of the present work is to prepare new water soluble materials based on rosin having high performance at lower concentrations as corrosion inhibitors in acid media. The objective of this work is to investigate the corrosion behavior of mild steel in 1M HCl solution in presence of the new modified cationic surfactant based on rosin by different electrochemical techniques.

2. EXPERIMENTAL

2.1. Materials

All materials were used without further purification. Rosin acid (AbA) with acid number 165 mg KOH · g^{-1} was obtained from a commercial resin by crystallization from cooled concentrated acetone solutions and purified by recrystallization from the same solvent. The separation of the resin acids from rosin was carried out to increase the yield and to remove terpens. Maleic anhydride, 2-diethylethanolamine, hexadecyl bromide, tetrahydrofuran (THF), acetate acid, petroleum ether, ethyl acetate, triethylamine (TEA) and oxalyl chloride ($C_2Cl_2O_2$) were purchased from Aldrich Chemical Co.

2.2. Preparation

2.2.1. Preparation of maleopimaric acid (MPA)

Gum rosin (0.33 mol; 100 g) was heated to 180 ^{o}C and maintained at this temperature for 1 h under the nitrogen atmosphere. Maleic anhydride (0.31 mol; 30 g) was then added and stirred at 180 ^{o}C for 3 h followed by raising the temperature to 220 ^{o}C and maintaining for 1 h. The reaction was cooled to 100 ^{o}C and 200 ml acetic acid was added. The white solid powder (crude MPA) was obtained after

cooling. The crude product was recrystallized twice from acetic acid and obtained yield of 45 % (55 g) as white crystal.

2.2.2. Preparation of rosin diethylaminoethyl ester (RMAE):

MPA(10 g, 0.025 mol) was dissolved in 50 ml toluene and added to a round bottom flask. Oxalyl chloride (2.95 ml , 0.03 mol) 50% solution in toluene was added slowly and the reaction mixture stirred at 95-98 ^{o}C for 4 h. The HCl gas liberated in the reaction was absorbed by base solution. After removed of the unreacted oxalyl chloride by vacuum distillation, the MPA chloride was obtained. Toluene (50 ml) , 2-diethylaminoethanol (1.46 g,0.025 mol) and triethylamine (3.5 ml , 0.025 mol) were then added into the flask. The mixture was stirred refluxed at temperature of 98 ^{o}C for 6 h. Then the mixture was filtered, and filtrate was washed with waters to neutral the reaction filtrate and dried. Toluene was removed under reduced pressure; the corresponding rosin diethylaminoethyl ester was obtained in 80 % yield.

2.2.3. Preparation of rosin cationic surfactants (QRMAE):

To prepare quaternary amine of rosin diethylaminoethyl ester, a similar flask was charged with 10 g of appropriate amino ester, after which 100 g of hexadecyl bromide was added in portions with stirring. Quaternization was performed at 85 -90 ^{o}C for 5 hrs. Excess of hexadecyl bromide was removed after distilled under reduced pressure. Then the mixture was extracted by ether and water three times. Aqueous phase remained and distilled under reduced pressure for recrystallization from alcohol and acetone. The corresponding quaternary amine of diethylaminoethyl rosin ester was obtained in 85 % yield.

2.3. Characterization:

FTIR spectra were analyzed with a Nicolet FTIR spectrophotometer using KBr in a wavenumber range of 4000–500 cm-1 with a resolution accuracy of 4 cm $^{-1}$. All samples were ground and mixed with KBr and then pressed to form pellets.

^{1}H-NMR (400 MHz Bruker Avance DRX-400 spectrometer) was used to investigate the chemical structures of the prepared rosin derivatives using $CDCl_3$ as solvent and tetramethylsilane (TMS) as an internal reference.

The surface tension measurements of different aqueous solution of the prepared quaternary amine of diethylaminoethyl rosin ester in water and 1M HCl was measured at 25 ^{o}C by means of the pendent drop technique using drop shape analyzer model DSA-100 (Kruss, Germany). The error limits of these measurements are on the order of 0.1 mN/m or less. Pendent drops were formed on the tip of a Teflon capillary with an outside diameter of 0.1 in. and inside diameter of 0.076 in.

2.4. Electrochemical measurement:

A standard three-electrode electrochemical/corrosion cell was utilized in all electrochemical experiments. The counter electrode was a platinium electrode. The reference electrode was a Ag/AgCl. The working electrode was prepared from a carbon steel (CS) sealed with an exposed area (0.1 cm^2) to the electrolyte. Electrochemical measurements and EIS impedance measurements were performed using a Solartron 1470E system (potentiostat/galvanostat) with Solartron 1455A as frequency response analyzer. Multistate software was used to run the tests, collect and evaluate the experimental data. Impedance tests were performed in 1M HCl with and without inhibitor. The impedance data were analyzed and fitted with the simulation ZView 3.3c , equivalent circuit software.

3. RESULTS AND DISCUSSION

3.1. Synthesis of quaternary amine of diethylaminoethyl rosin ester:

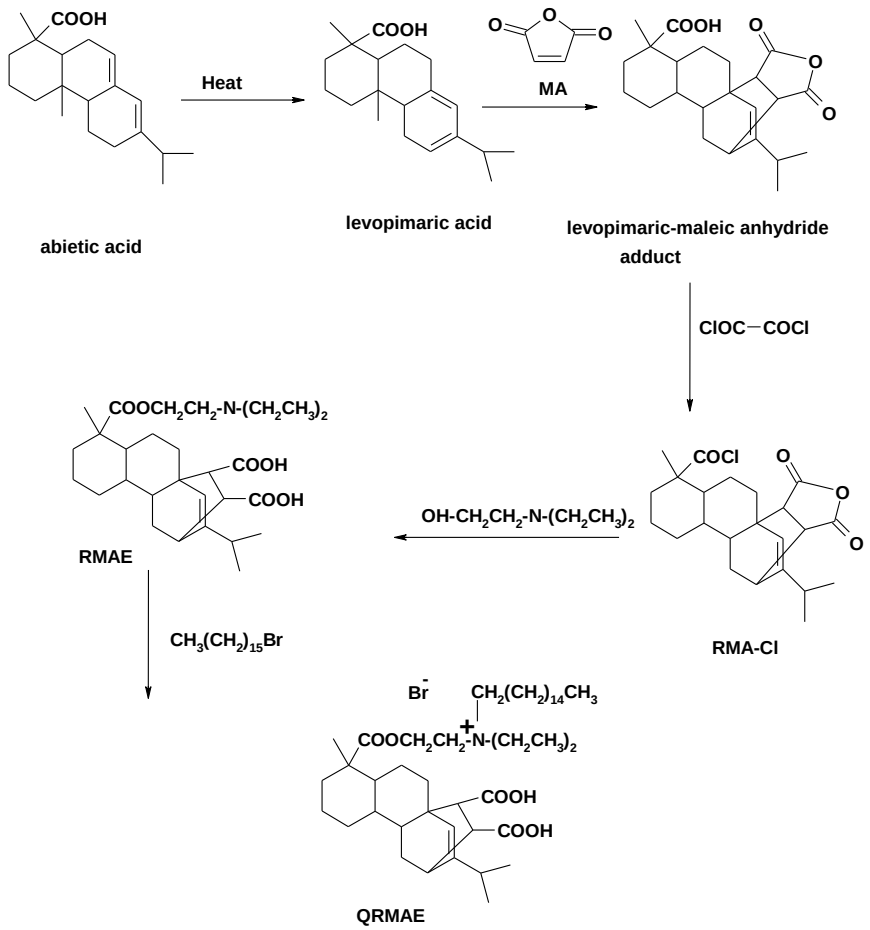

Scheme 1. Scheme of reaction to obtain QRMAE cationic surfactant.

The present work aims to prepare cationic surfactants by quaternization of rosin diethylaminoethyl ester with hexadecyl bromide. The reaction scheme was illustrated in scheme 1. In this respect, Diels-Alder reaction completed between maleic anhydride and rosin acid after

isomerization of rosin acid to levopimaric acid under the heat or acid condition [17]. Gum rosin was used as starting material to synthesize the MPA, which can decrease the cost, while compared to the employment of abietic acid. Gum rosin was heat to 180 ^{o}C and carried out the isomerization so that other resin acid would convert to levopimaric acid prior to Diels-Alder reaction with maleic anhydride.

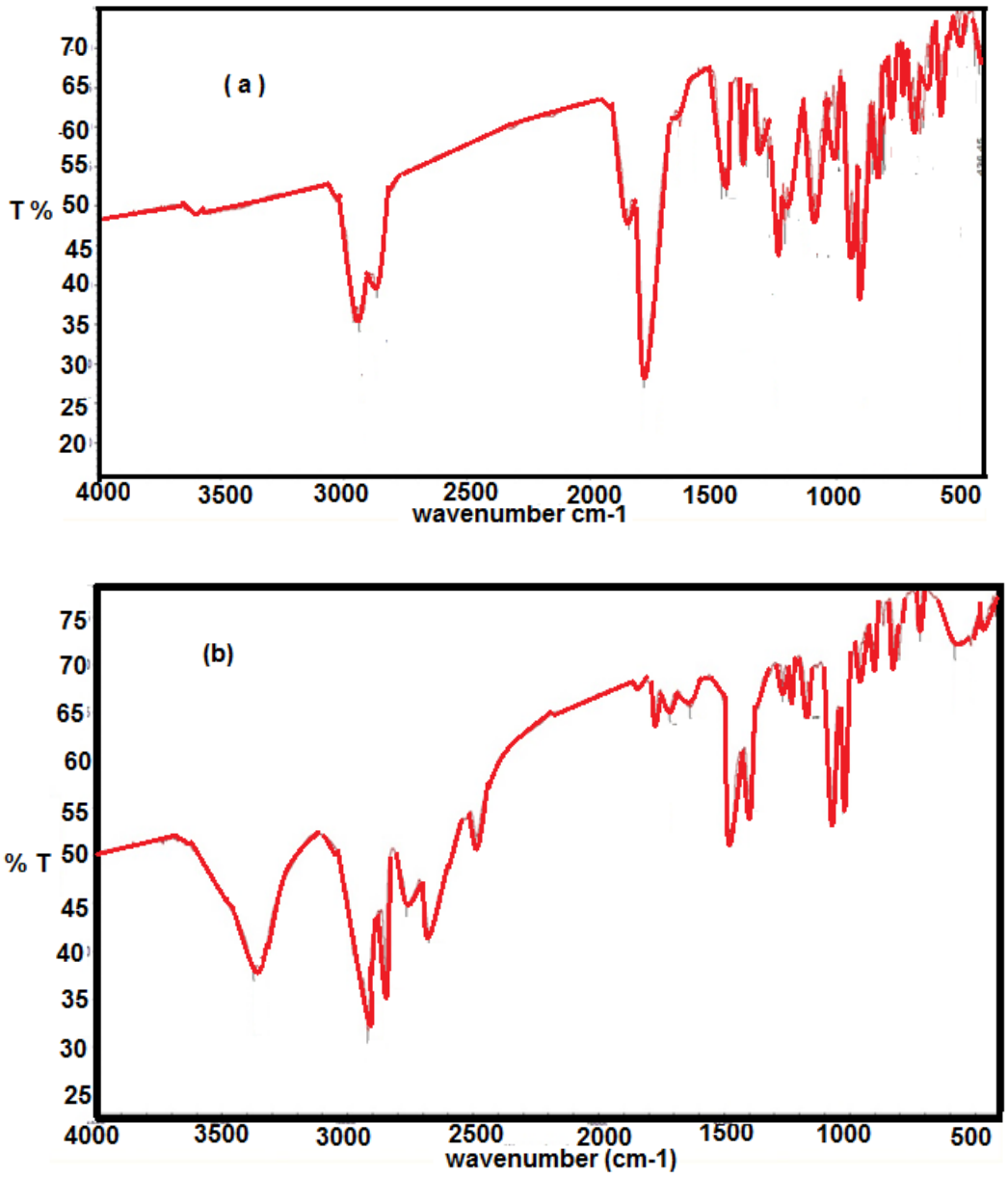

Figure 1. FTIR spectra of a) RMAE and b) QRMAE.

The successful synthesis of MPA was rectified by the FTIR spectrum of MPA and showed that the formation of anhydride group is evidenced by the absorption bands at 1842cm^{-1} and 1778 cm^{-1}. The presence of preexisting carboxyl group from the resin acid is reflected by the absorption at 1693 cm^{-1}. The structure and purity of MPA were also confirmed by ^{1}H NMR (500 MHz, $CDCl_3$) δ: 5.54 (s, 1H,

C*H*=C); 3.10 (d, 1H, C*H*C=O); 2.73 (d, 1H, C*H*C=O); 2.5 (d, 1H, C*H*C=CH); 2.27 (m, 1H, CC*H*(CH3)2).

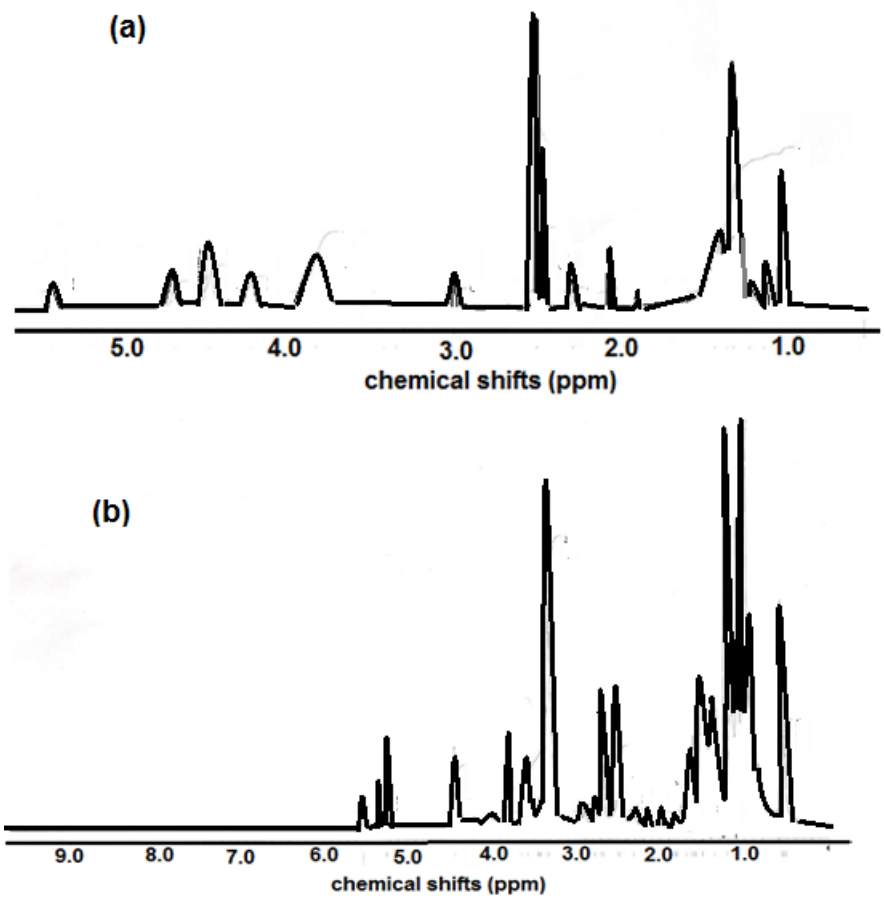

Figure 2. 1HNMR spectra of a) RMAE and b) QRMAE.

Due to the steric effect of MPA moiety, the quaternization of MPA was carried out with two steps. The carboxyl group of MPA was converted to acyl chloride and then reacted with diethyletanolamine in present of catalyst triethylamine. FTIR spectrum of rosin diethylaminoethyl ester (figure1a) confirmed the appearance of new absorption peak at 1729 cm^{-1} and the disappearance of band at 3450 cm^{-1} , which arised from the ester (carbonyl group) and OH stretching of COOH, respectively, indicated that diethyletanolamine has successfully esterified with MPA (scheme 1). The structure and purity of rosin ester was further confirmed by ^{1}H NMR. ^{1}H NMR spectrum represented figure 2a (500 MHz, $CDCl_3$) δ: 5.54 (s, 1H, C*H*=C); 4.61 (t, 2H, OCH_2-C); 4.21 (q, 4H, NCH_2-C); 3.10 (d, 1H, C*H*C=O anhydride); 2.73 (d, 1H, C*H*C=O anhydride); 2.5 (d, 1H, C*H*C=CH); 2.27 (m, 1H, CC*H*$(CH_3)_2$); 0.84 (m, 12H, C-$(CH_3)_2$ and (C-$CH_3)_2$).

The chemical structure of quaternized rosin diethylaminoethyl ester was confirmed also by FTIR and ^{1}HNMR analyses which represented in figures 1b and 2b, respectively. The appearance of new broad absorbance band, Figure 1b) at 3430 cm^{-1} and disappearance of 1810 and 1780 cm^{-1} (C=O of anhydride group) in the chemical structure of quaternized rosin diethylaminoethyl ester confirmed the anhydride five-membered ring of MPA opened and -OH is produced. Appearance of peak around

1371 cm^{-1} was assigned to C-N stretching vibration. Due to the quaternization (Figure 2b), a small intense peak at 2365.72 cm^{-1} has appeared, which is the characteristic absorption peak of quaternary ammonium groups. Some structural changes takes place in the reactant rosin diethylaminoethyl ester. Appearance of new peaks (figure 2b) at 1.3 δ is assigned to the $(CH_2)_{15}$ protons from hexadecyl group. From all these evidences, it is clear that quaternization of rosin diethylaminoethyl ester have been successfully carried out in the rosin diethylaminoethyl ester unit at ethyl amine group.

3.2. Surface Activity of the prepared surfactants

It was previously concluded that [15] the surface tension of the aqueous nonionic surfactant solutions was not affected by 1 M HCl. While the data of critical micelle concentrations (cmc) were reduced by 1MHCl. In the present work the surface tension of the prepared rosin cationic surfactant will be evaluated in both distilled water and 1 M HCl to study the adsorption characteristics at air/water interface and micellization of the cationic surfactants in bulk solutions either in distilled or acidic aqueous solutions.

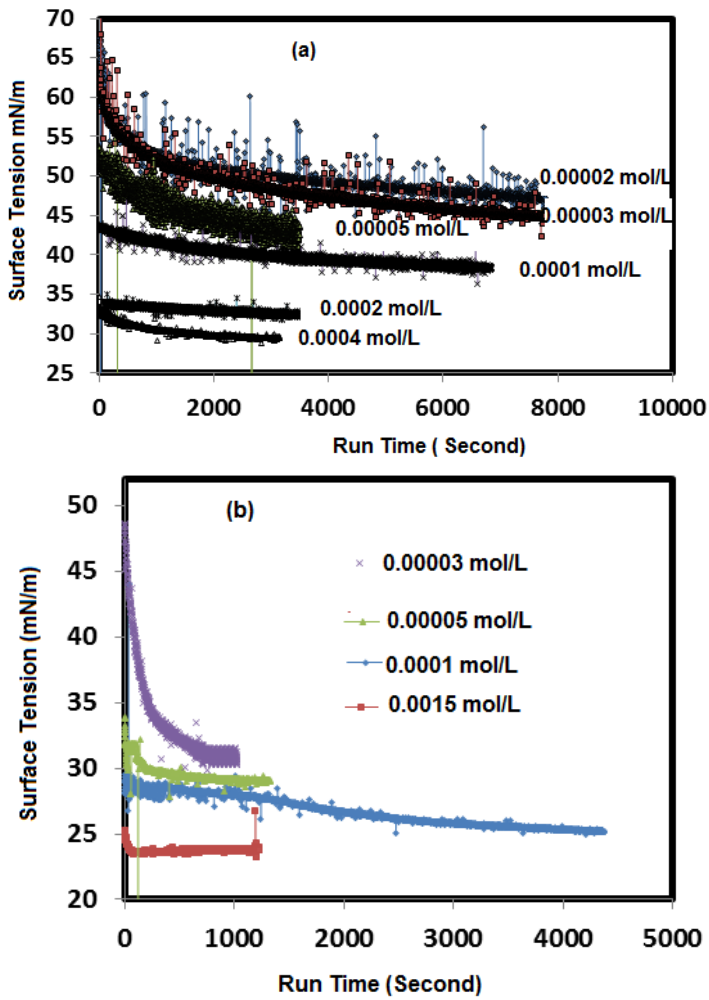

Figure 3. Relation between surface tension of QRMAE and time at different concentrations in a) water and b) 1M aqueous HCl solutions at 25 ^{o}C.

In the present work, the dynamic surface tension for different concentrations of the prepared surfactant was measured at water/air interface at temperature of 25 ^{o}C. The relation between the surface tension of QRMAE in aqueous and 1 M HCl aqueous solutions and time at different concentrations were represented in figure 3 a and b, respectively. The adsorption isotherms of the prepared surfactant QRMAE in water and aqueous solution1M at temperature of 25 ^{o}C were plotted in figure 4 a and b, respectively.

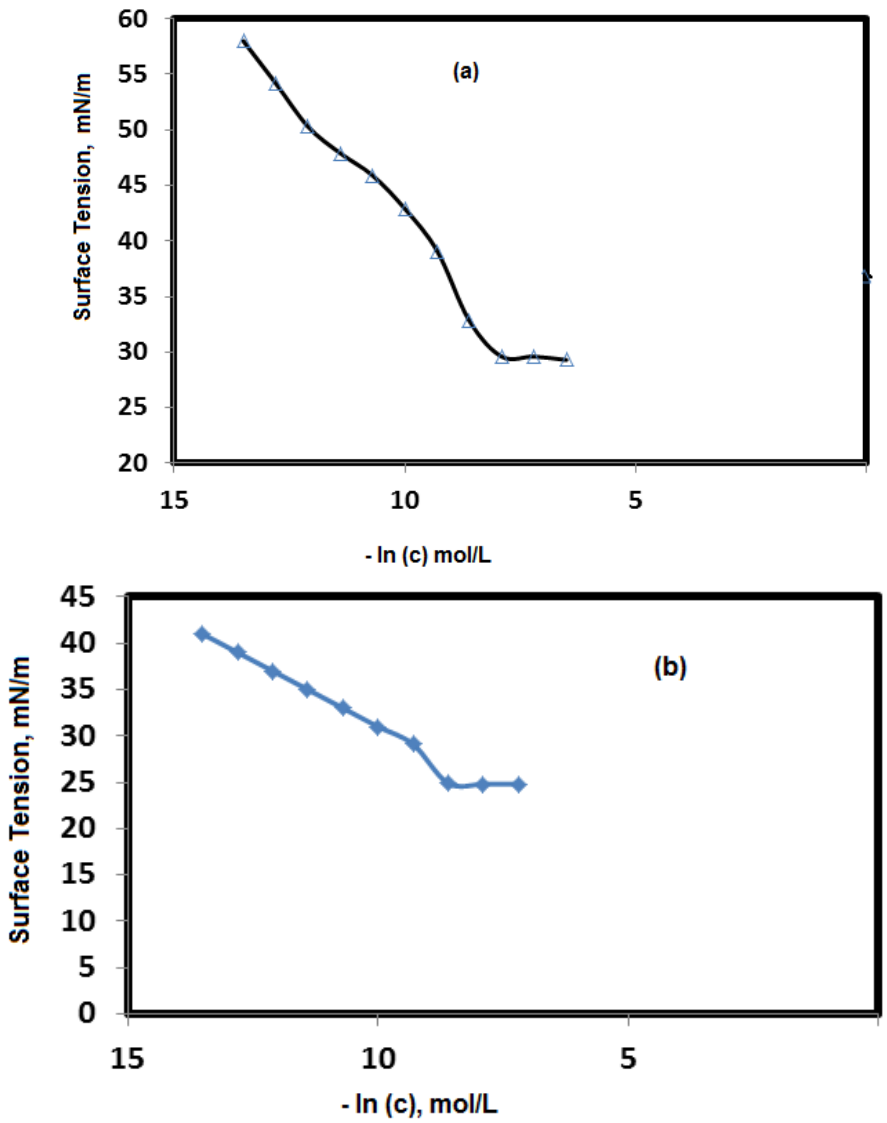

Figure 4. Adsorption isotherms of QRMAE at different concentrations in a) water and b) 1M aqueous HCl solutions at 25 ^{o}C.

The data represented in figure 3 a and b indicated that the prepared surfactants reached the surface tension equilibrium after time intervals ranged from 5 to 30 minutes. Moreover, the equilibrium time was reduced with increasing the surfactant concentrations and replacement of water with 1M HCl. These data indicated that the prepared surfactants are strongly adsorbed at interfaces in 1M HCl solutions. It is well known that the micellization, aggregation and adsorption of surfactants are

based on the critical micelle concentrations (cmc), which were determined by the surface balance method as represented in figure 4. The cmc data of QRMAE were determined in water and 1 M HCl aqueous solution at 25 ^{o}C from abrupt changes of the plotted data of surface tension (γ) versus the solute concentration (ln C) and listed in table 1.

Table 1. Surface activity data of QRMAE in water and 1M HCl at 25 ^{o}C.

Medium	Cmc x 10^4 mol/L	γ_{cmc} mN/m	$\Delta\gamma$ mN/m	$(-\partial \gamma / \partial \ln c)_T$	Γ_{max} x 10^{10} mol/ cm^2	A_{min} nm^2 /molecule
water	4.2	29.4	42.7	4.91	2.05	0.081
1M HCl	2.1	24.7	47.4	3.09	1.29	0.129

On the other hand, the surface activity data of QRMAE such as the surface tension at cmc, γ_{cmc}, effectiveness of the prepared surfactants expressed by the maximum reduction of surface tension which calculated from the equation, $\Delta\gamma = \gamma_{water} - \gamma_{cmc}$, the concentration of the prepared surfactants at the solvent–air interface, Γ_{max}, and the area per molecule at the interface, A_{min}, were calculated and listed in table 1. The surface excess concentration of the prepared surfactants at the interface can be calculated from surface or interfacial tension data using the following equation: $\Gamma_{max} = 1/RT \times (-\partial \gamma / \partial \ln c)_T$, where $(-\partial\gamma / \partial \ln c)$ T is the slope of the plot of γ versus ln c at constant temperature (T), determined from figure 4, and R is the gas constant (in J mol^{-1} K^{-1}). The Γ_{max} values were used for calculating the minimum area Amin at the aqueous–air interface. The area per molecule at the interface provides information on the degree of packing and the orientation of the adsorbed surfactants, when compared with the dimensions of the molecule as obtained from models. From the surface excess concentration, the area per molecule at the interface is calculated using the equation: $A_{min} = 10^{16}/ N \Gamma_{max}$, where N is Avogadro's number. The data listed in table 1 indicated that the cmc values were reduced from 0.0004 to 0.0002 mol/L in aqueous 1M HCl which can be attributed to the lower solubility of QRMAE cationic in acid solution. It was previously concluded that, decreasing the cmc values indicated the high tendency of the surfactants to adsorb at the liquid interfaces [22]. Also, it is increased their area occupied at the interface [23]. These data indicated that the prepared QRMAE cationic surfactant favor micellization in bulk 1M HCl solution than aqueous solution which may reflect to its greater tendency to adsorb at metal liquid interface more than air/water interface.

3.3 Polarization measurements

Polarization curves for carbon steel in 1M HCl in absence and presence of cationic inhibitor with different concentrations (50-250 ppm) are shown in Fig.5 As can be seen the cathodic curves were more polarized than anodic curves where the cathodic reaction is remarkably affected by the inhibitors, whereas the anodic one is slightly shifted toward lower currents. It can also be seen that the anodic and cathodic reactions were inhibited more and the corrosion currents reduced to lower values.

The corrosion current density (icorr) obtained from the polarization curves for carbon steel in absence and presence of various concentrations of cationic derivatives in 1M HCl are listed in Table 2.

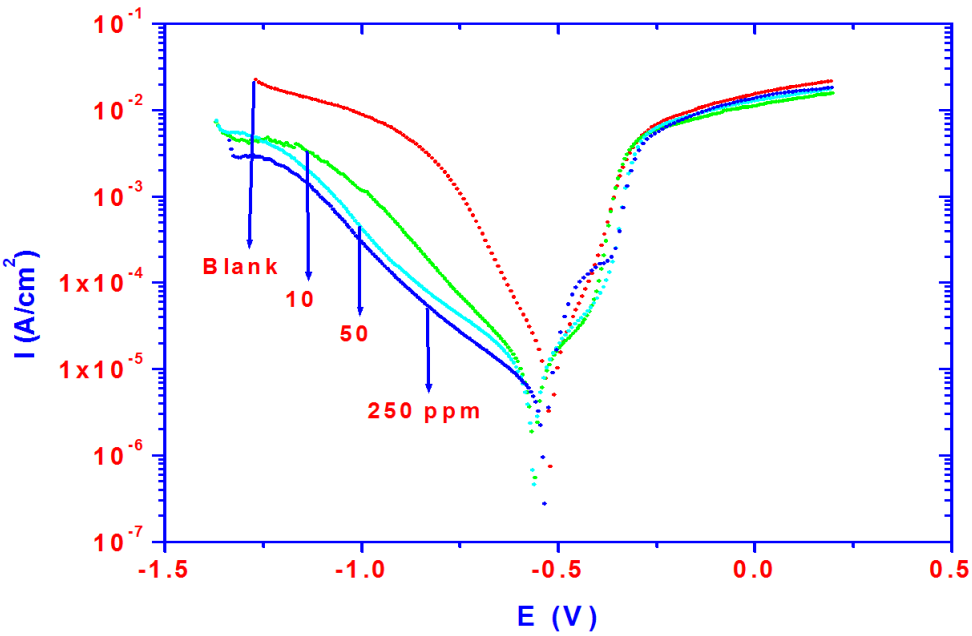

Figure 5. Polarization curves for carbon steel in 1M HCl solution containing different inhibitor concentration.

Table 2. Inhibition efficiency values for carbon steel in 1M HCl with different concentrations of cationic calculated by EIS technique.

Inhibitor conc. (ppm)	R_{ct}	EI % EIS technique
10	201.8	71.3
50	554	89.53
100	785	92.62

It is clear that the addition of cationic inhibitor influenced the cathodic and anodic reactions. It controls the rate of hydrogen evolution reaction on steel surface as well as the anodic dissolution. The inhibition efficiency was evaluated from icorr and listed in Table 3 using the following equation [24]:

$$IE(\%) = i^{o}_{corr} - i_{corr} / i^{o}_{corr}$$

where i^{o}_{corr} and i_{corr} are the corrosion current densities for carbon steel electrode in the uninhibited and inhibited solutions, respectively. It is clear that cationic species in 1 M HCl medium, may be adsorbed on the cathodic sites of the mild steel and reduce the evolution of hydrogen. Moreover, the adsorption of this compound on anodic sites will then reduce the anodic dissolution of carbon steel. The data presented in Table 2 revealed that the corrosion current density (icorr)

decreases considerably with increasing cationic concentration. It can be concluded that the addition of cationic leads to blocking the available cathodic and anodic sites on the steel surface. Thus, causes a decrease in the exposed area for hydrogen evolution as well for anodic dissolution. The dependence of IE (%) versus the inhibitor concentration of cationic is also presented in Table 2. The obtained efficiencies indicate that cationic acts as effective inhibitor with maximum efficiency value (92 %) at 250 ppm concentration. From Table 2, it can also be seen that cationic inhibits the carbon steel corrosion to a large extent and the inhibition efficiency is dependent on the inhibitor concentration. The cationic molecules were first adsorbed on the steel surface and blocked the reaction sites of the carbon steel surface and is accompanied by a reduction in avaliable the surface area for H+ ions reduction and anodic dissolution, while the actual reaction mechanism remains unaffected [25]. A higher coverage of the cationic on the surface was obtained in solutions with the higher concentrations (250 ppm).

3.4. Electrochemical impedance spectroscopy (EIS)

In order to obtain information about the kinetics of carbon steel corrosion in presence of cationic inhibitor, the electrochemical process taking place at the open-circuit potential was examined by electrochemical impedance spectroscopy (EIS). The recorded EIS spectrum for steel in 1 M HCl (Fig. 6) showed one depressed capacitive loop. The same trend (one capacitive loop) was also noticed for mild steel immersed in 1 M HCl containing cationic (50–250 ppm) as shown in Fig. 7. The diameter of Nyquist plots increased on increasing the concentration of cationic indicating strengthening of inhibitive film. Electrical equivalent circuits shown in Fig. 8 are generally used to model the electrochemical behaviour and calculate the parameters of interest such as electrolyte resistance (Rs) and charge transfer resistance (Rct).

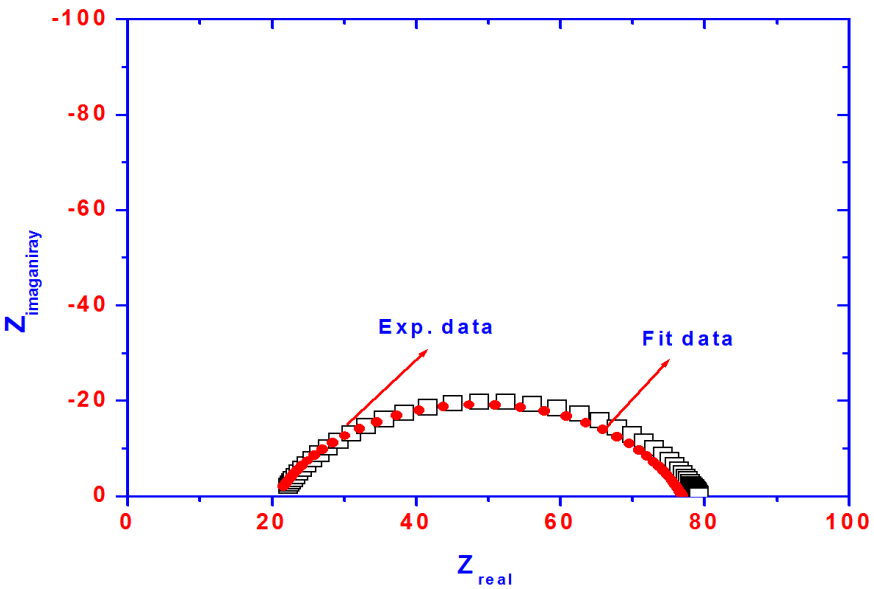

Figure 6. Nyquist diagram for carbon steel in 1 M HCl solution.

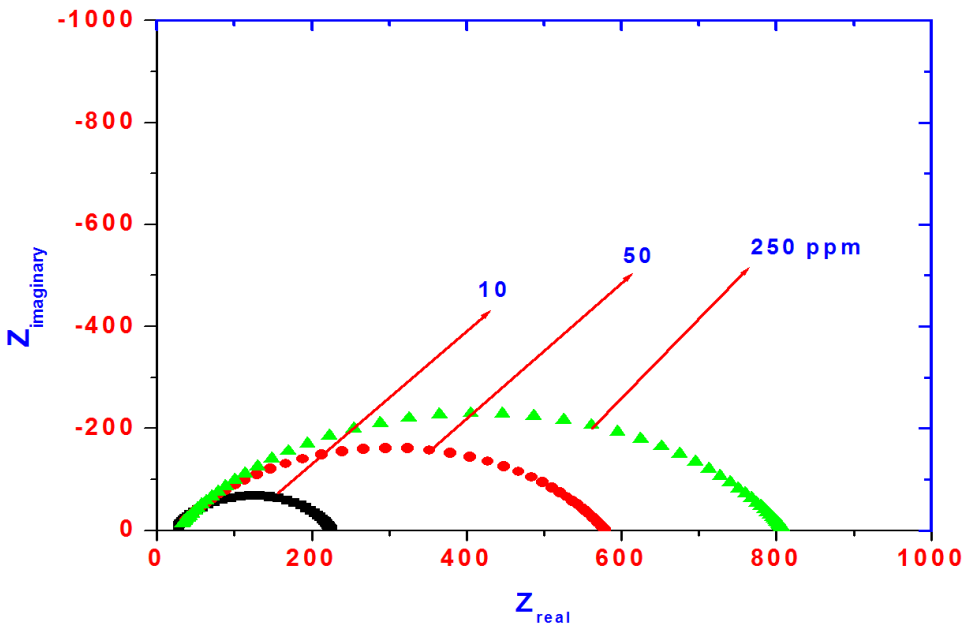

Figure 7. Nyquist diagram for carbon steel in 1 M HCl containing different concentration of inhibitors.

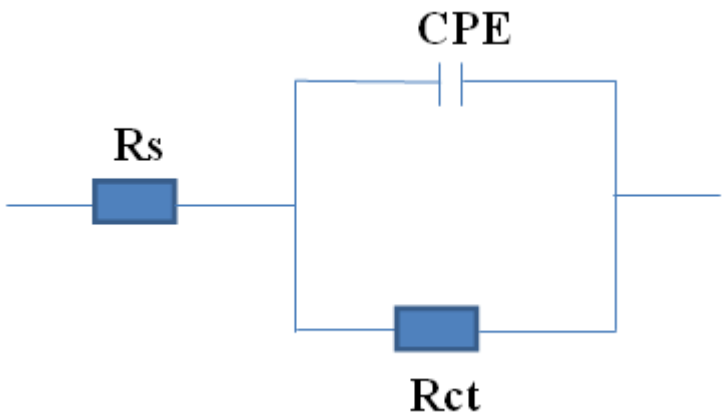

Figure 8. Equivalent circuit used for fitting the impedance data in 1 M HCl solution.

The above impedance diagram (Nyquist) contains a depressed semicircle with the center under the real axis, such behavior is characteristic for solid electrode which is attributed to surface roughness and inhomogeneities of metal electrodes. For the description of a frequency independent phase shift between an applied alternating potential and its current response, a constant phase element (CPE) is used instead of capacitance (C). The CPE is defined by the mathematical expression [26,27]

$Z_{CPE} = 1 / A (j\square)^n$

where Z (CPE), impedance of CPE; A, a proportional factor; □, angular frequency; j is √-1; n, surface irregularity.

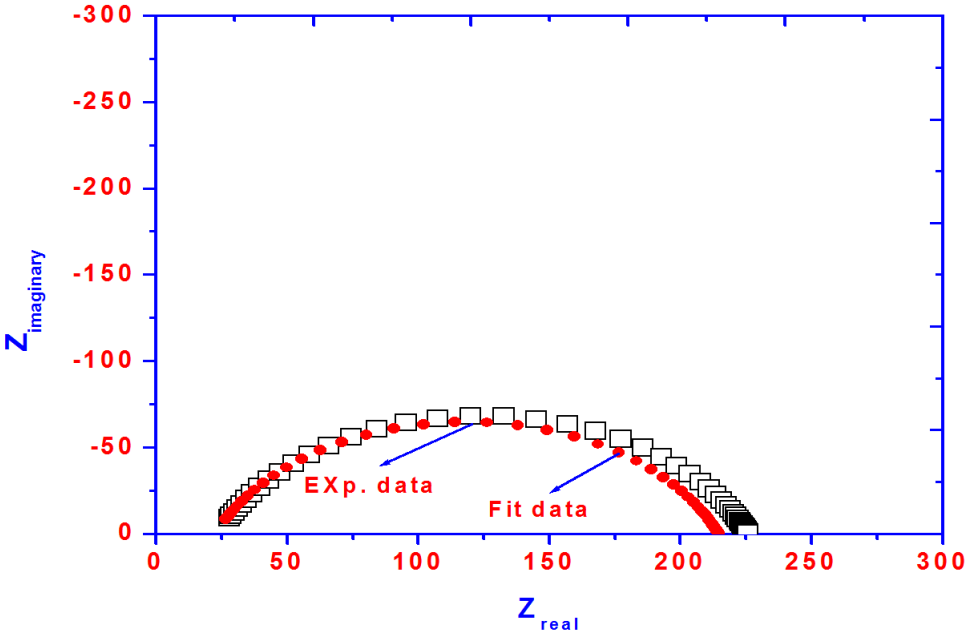

Figure 9. Nyquist diagram for carbon steel in 1 M HCl containing 10ppm concentration of inhibitor showing experimental and fitting data.

The CPE, which is considered a surface irregularity of the electrode, causes a greater depression in Nyquist semicircle diagram [26], where the metal– solution interface acts as a capacitor with irregular surface. If the electrode surface is homogeneous and plane, the exponential value (n) becomes equal to 1 and the metal–solution interface acts as a capacitor with regular surface, i.e. when n = 1, A = capacitance. Simulation of Nyquist plots with Randle's model containing constant phase element (CPE) instead of capacitance and charge transfer resistance (Rct) showed excellent agreement with experimental data. The main parameters deduced from the analysis of Nyquist diagram for 1 M HCl containing various concentrations of cationic are given in Table 2. On increasing cationic concentration, the charge transfer resistance (Rct) increased and capacitance (A) decreased indicating that increasing cationic concentration decreased corrosion rate. Decrease in the capacitance was caused by reduction in local dielectric constant and/or by increase in the thickness of the electrical double layer. This fact suggests that the inhibitor molecules acted by adsorption at the metal/solution interface [28]. The lower value of n for 1 M HCl medium indicated surface inhomogeneity resulted from roughening of metal surface due to corrosion. Addition of cationic (250 ppm) reduces the surface inhomogeneity due to the adsorption of cationic molecules. As the concentration of cationic inhibitor increased, the Rct values increased indicating decrease in the formation of anodic process controlling intermediates from anodic dissolution and subsequently inhibition of corrosion. The maximum Rct values were achieved for 250 ppm. Fig. 9 shows the Nyquist plot of the experimental and fit data for carbon steel containing 10ppm of inhibitor concentration.

Table 3. Inhibition efficiency values for carbon steel in 1M HCl with different concentrations of cationic calculated by polarization method.

Inhibitor conc. (ppm)	i_o x 10^{-5}	EI % Polarization method
10	0.662	56.44
50	0.301	80.19
100	0.193	87.30

The results of polarization measurements (Tables 2) are in acceptable agreement with those obtained from EIS (Table 3) study and show the same trend.

4. CONCLUSIONS

The following conclusion can be extracted from the previous results:

1. We succeeded to prepare new cationic rosin QRMAE based on rosin and its chemical structure confirmed by IR and ^{1}HNMR analyses.
2. The surface activity data indicated that the prepared QRMAE cationic surfactant favor micellization in bulk 1M HCl solution than aqueous solution which may reflect to its greater tendency to adsorb at metal liquid interface more than air/water interface.
3. Cationic molecules show excellent inhibition properties for the corrosion of carbon steel in 1 M HCl and the inhibition efficiency increases with increase in the inhibitor concentration.
4. The results of EIS indicate that the value of charge transfer resistance tends to increase by increasing the inhibitor concentration.

ACKNOWLEDGMENT
The authors extend their appreciation to the Deanship of Scientific Research at King Saud University for funding this work through research group no RGP-VPP-235.

References

1. M. Lagrnee, B. Mernari, M. Bonanis, M. Traisnel, F. Bentiss, *Corros. Sci.* 44 (2002) 573.
2. D. Tayaperumal, S. Muralidharan, G. Venkatchari, N.S. Rengaswamy, *Anti-corros. Method Mater.* 47 (2000) 349.
3. A. M. Atta, M. El-Sockary, S. AbdelSalam, *Prog. Rubber, plastics and Recycliing Technol.* 23(4) (2007) 241.
4. M. Attia, A. M. Hasan, A. M. Atta, *Materials Chem.Physics* 121 (2010) 208–214.
5. A. M. Atta, O. E. El-Azabawy, H.S. Ismail, *Corrosion science* 53 (2011)1680.
6. I. L. Rosenfeld, Corrosion Inhibitors, McGraw-Hill, New York, 1981.
7. P. Kutej, J. Vosta, J.J. Pancir, N. Hackerman, *J. Electrochem. Soc*. 142 (1995) 1847.
8. S.L. Granese, B.M. Rosales, C. Oviedo, J.O. Zerbino, *Corros. Sci*. 33 (1992) 1439.
9. J. Zhang, *Rosin Based Chemicals and Polymers*, A Smithers Rapra Technology Ltd., UK (2012).
10. 10. J.Li, X. P. Rao, S. B. Shang, Y. Q. Gao, J. Song, *BioResources* 7(2) (2012)1961-1971.

11. J. F. Wang, Y. P. Chen, K. J.Yao, P. A. Wilbon,. *Chem. Commun.* 48(6) (2012) 916-918.
12. Y. Zheng, K. Yao, J. Lee, D. Chandler, J. Wang, C. Wang, F. Chu, C. Tang, *Macromolecules* 43 (2010) 5922.
13. A. M. Atta, A. M. Elsaeed, *J. Appl. Polym. Sci.* 122 (1) (2011)183.
14. A.M. Atta, G. A. El-Mahdy, H. S. Ismail, H.A. Al-Lohedan *Int. J. Electrochem. Sci.*, 7 (2012) 11834.
15. G. A. El-Mahdy, A.M. Atta, H. A. Al-Lohedan, *Int. J. Electrochem. Sci.*, 8 (2013) 5052 - 5066.
16. A. M. Atta, G. A. El-Mahdy, A. A. Al-Azhary, H. A. Al-Lohedan *Int. J. Electrochem. Sci.*, 8 (2013) 1295.
17. A.M. Atta, A.M. Ramadan, K. A. El-Shafay, A. M. Mohamed, N.S. Ragab, M. Fekry, *J. Disp. Sci. Technol.* 30 (2009)1100.
18. 18. A.M. Atta, M. E. Abdel-Rauf, N. E. Maysour, A. K. Gafer, *J. Disp. Sci. Technol.* 31 (2010)583–595.
19. A.M. Atta, R. Mansour, M. I. Abdou, A. M. Sayed. *Polym. Adv. Technol.* 15 (2004) 514.
20. A. M. Atta, S.M. El-Saeed, R. K. Farag, *React. Funct. Polym*. 66 (2006) 1596.
21. A. M. Atta A. M. Elsaeed, R.K. Farag, S. M. El-Saeed *React. Funct. Polym*. 67 (2007)549.
22. D. Asefi, M. Arami, A.A. Sarabi, N.M. Mahmoodi, *Corros. Sci.* 51 (2009) 1817.
23. N.A. Negm , A.M. Al Sabagh, M.A. Migahed, H.M. Abdel Bary, H.M. El Din, *Corrosion Science* 52 (2010) 2122.
24. F.Z. Bouanis, F. Bentiss, M. Traisnel, C. Jama, *Electrochim. Acta* 54 (2009) 2371.
25. R. Solmaz, G. Kardas, M.C. Ulha, B. Yazıcı, M. Erbil, *Electrochim. Acta* 53 (2008) 5941.
26. J. Cruz, T. Pandiyan, E.G. Ochoa, *J. Electroanal. Chem*. 583 (2005) 8.
27. D.A. Lopez, S.N. Simison, S.R. de Sanchez, *Corros. Sci*. 47 (2005) 735.
28. H.A. Sorkhabi, B. Shaabani, D. Seifzadeh, *Electrochim. Acta* 50 (2005) 3446.

© 2013 by ESG (www.electrochemsci.org)